Laser and Particle Beams (2017), *35*, 551–560.

doi:10.1017/S0263034617000544

Reflected and transmitted second harmonics generation by an obliquely *p*-polarized laser pulse incident on vacuum-magnetized plasma interface

M. GHORBANALILU[1] AND Z. HEIDARI[2]

[1]Physics Department, Shahid Beheshti University, G. C., Tehran, Iran
[2]Physics Department of Azarbaijan Shahid Madani University, Tabriz, Iran

(RECEIVED 17 May 2017; ACCEPTED 13 July 2017)

Abstract

The transmitted and reflected second harmonics (SH) generation by an oblique *p*-polarized laser pulse irradiated on vacuum-magnetized plasma interface is investigated. The laser pulse propagates through a homogenous, underdense, and transversely magnetized plasma. The transverse magnetic field plays the role of a self-generated magnetic field produced in laser plasma interaction. It is shown that if the transmitted and reflected SH components investigated as a simultaneous process, the maximum SH power deviates from previous reports specially near the critical angle. The deviation increases with laser field intensity and plasma density. The results reveal that the conversion efficiency increases slightly by increasing incident angle and drastically enhances near the critical angle. We show that the transmitted SH power decreases by increasing the magnetic field strength, in contrast to the normal incidence, which the SH power is increased. The comparison revealed that the SH efficiency is greater for transmitted component, while the reflected component is more proper for technical and experimental applications. This paper not only conforms the previous reports for angle far from the critical but also modifies them for the SH generation near the critical angle. Moreover, this paper gives a new insight for SH generation by a magnetized plasma.

Keywords: Harmonic generation; Laser plasma interaction; Magnetized plasma

1. INTRODUCTION

The problem of intense short-pulse laser–plasma interaction has been an active area of research. Among them, non-linear phenomenon of harmonic generation has been interested by many researchers from 1961 up to now (Franken *et al*., 1961; Grebogi *et al*., 1983; Esarey *et al*., 1993; Ondarza-Rovira & Boyd, 2000; Földes *et al*., 2003; Racz *et al*., 2006; Cairns, 2009). In process of high-order harmonic generation, second harmonics (SH) has a unique place because of many applications such as extreme ultraviolet non-linear optics (Yeung *et al*., 2017), laser–plasma interaction properties, X-ray sources (Giulietti *et al*., 2009), etc. On the other hand, the generation of magnetic fields during high-intensity laser–plasma interaction is a subject that has been under investigation for many years (Lehner, 1994; Berezhiani *et al*., 1997; Gorbunov *et al*., 1997; Zheng *et al*., 2000; Kato *et al*., 2004). This subject has motivated an ingoing strong effort to analysis of laser interaction with magnetized plasmas.

A magnetic field with proper configuration may be employed for efficient SH generation by providing the additional momentum, which is essential for phase matching (Kant & Sharma, 2004; Askari & Noroozi, 2009, 2011; Vaziri (Khamedi) *et al*., 2015). When a magnetic field is applied into a plasma, the electron dynamic is modified, and this leads to the non-linear current modification. Therefore, it is reasonable that the magnetic field affects the harmonics generation. The magnetic field could have additive (Kant & Thakur, 2016) or destructive (Sharma & Sharma, 2012; Kuri & Das, 2016) role on SH conversion efficiency in interaction of laser-magnetized plasma. When the density perturbation produced by magnetic field is coupled with electron quiver motions, it is plausible to generate the SH (Jha *et al*., 2007). It has been shown that the SH power is increased by increasing the magnetic field strength in normal

Address correspondence and reprint requests to: M. Ghorbanalilu, Physics Department, Shahid Beheshti University, Evin, Tehran, Iran. E-mail: m_alilu@sbu.ac.ir & mh_alilo@yahoo.com

radiation of a linearly polarized laser pulse with a magnetized plasma; however, the magnetic field was essential for SH generation. On the other hand, when a *p*-polarized laser pulse is obliquely incident on a vacuum–plasma interface, SH can be generated in the absence of magnetic field and or any required conditions for phase matching (Jha & Agrawal, 2014). Generation of phase-mismatch second and third harmonics has been studied in the interaction of an intense laser pulse with strongly magnetized dense plasma, and it is shown that the harmonic efficiencies can be increased by magnetic field (Ghorbanalilu, 2012). In addition, generation of phase-mismatch SH radiation in the reflected component of vacuum–plasma interface by using a *s*-polarized laser pulse have been reported (Parashar & Sharma, 1998; Singh *et al*., 2005).

The experimental and theoretical investigation approved strong SH generation in Argon gas by focused spatiotemporal femtosecond laser pulses (Li *et al*., 2014). On the other hand, second and third-harmonic generations from magnetic metamaterials have been observed under normal and oblique incidences of femtosecond Gaussian laser pulse (Klein *et al*., 2007). Furthermore, SH radiation from underdense plasma has already been observed in past decades (Mori *et al*, 2002; Giulietti *et al*., 2009). Moreover, the recent observation approves the SH generation in the laser interaction with plasma–vacuum boundary (Yeung *et al*. 2017).

The brief history of SH generation shows that this phenomena has been studied by many authors. They have investigated the SH generation inside the plasma or in the vacuum. In view of this fact that in a real physical system the SH can be generated inside the plasma as well as vacuum due to the laser pulse interaction with plasma surface, we would like to investigate the generation of SH in both sides of the plasma–vacuum boundary simultaneously. The results presented in this paper not only confirm the previous reports, but also can be modified and generalized to a magnetized plasma. On the other hand, results show that the SH power is less than that the previous reports for a non-magnetized plasma if the transmitted and reflected SH radiations are considered simultaneously. We show that deviation with previous reports enhances by increasing the laser intensity and plasma density. The model is valid for underdense plasma ($\omega_p^2/\omega_0^2 \ll 1$) in the weakly relativistic regime ($I_0 \leq 10^{17}$ W/cm^2 and or $a_0^2 \ll 1$) for angle of incidence varying from 0° up to critical angle. It is lucid that beyond the critical angle, propagation constant becomes imaginary number and the laser propagation becomes evanescent.

The organization of this paper is as follows: In the next section, we derive the equation for non-linear current density as a source of SH generation. The study is undertaken in the mildly relativistic regime, using a perturbative approach. In Section 3, we obtain the amplitudes of transmitted and reflected SH radiations. The SH conversion efficiency, for both transmitted and reflected components, is presented in Section 4, and the influences of incidence angle, magnetic field strength, and plasma density on SH power are investigated. The conclusion is summarized in Section 5.

2. FORMULATION AND GOVERNING EQUATIONS

Consider a vacuum–plasma interface at $z = 0$; $z < 0$ being vacuum and $z > 0$ a uniform underdense plasma of density n_0 that is set in a $\mathbf{B}(= B_0\hat{y})$ transverse magnetic field. A *p*-polarized laser beam (propagating in the *x*–*z* plane) incidents on the interface at an angle of incidence θ as shown in Figure 1.

$$E_0 = (\hat{x}\cos\theta - \hat{z}\sin\theta)\frac{1}{2}E_0\exp[i(k_{0x}x + k_{0z}z - \omega_0 t)] + c.c, \quad (1)$$

where E_0 is the amplitude of the incident electric field, $k_{0x} = (\omega_0/c)\sin\theta$ and $k_{0z} = (\omega_0/c)\cos\theta$ are the wavenumber components along the *x* and *z* directions, respectively. The electric and magnetic fields of the transmitted laser can be written as

$$E_1 = (\hat{x}(\epsilon_1 - \sin^2\theta)^{1/2} - \hat{z}\sin\theta)\frac{1}{2}E_1\exp[i(k_{1x}x + k_{1z}z - \omega_0 t)] + c.c, \quad (2)$$

$$B_1 = ck_1 \times E_1/\omega_0, \quad (3)$$

where $k_{1x} = k_{0x}$, $k_{1z} = (\omega_0^2/c^2\epsilon_1 - k_{1x}^2)^{1/2}$, and $\epsilon_1 = k_1^2c^2/\omega_0^2$ is the dielectric constant at frequency ω_0. $E_1 = 2\sqrt{\epsilon_1}E_0/(\epsilon_1 + \sqrt{\epsilon_1 - \sin^2\theta}/\cos\theta)$ is the amplitude of the fundamental electric field transmitted into the plasma. The SH electric field can be written as

$$E_2 = (\hat{x}(\epsilon_2 - \sin^2\theta)^{1/2} - \hat{z}\sin\theta)\frac{1}{2}E_2\exp[i(k_{2x}x + k_{2z}z - 2\omega_0 t)] + c.c, \quad (4)$$

where $k_{2x} = (2\omega_0\sin\theta)/c$, $k_{2z} = (4\omega_0^2/c^2\epsilon_2 - k_{2x}^2)^{1/2}$. Furthermore $\epsilon_2 = k_2^2c^2/4\omega_0^2$ and E_2 are the dielectric constants at frequency $2\omega_0$ and the SH wave amplitude, respectively. The wave equation governing the propagation of electromagnetic waves through the plasma is given by

$$\nabla^2\mathbf{E} - \nabla(\nabla.\mathbf{E}) - \frac{1}{c^2}\frac{\partial^2\mathbf{E}}{\partial t^2} = \frac{4\pi}{c^2}\frac{\partial\mathbf{J}}{\partial t}, \quad (5)$$

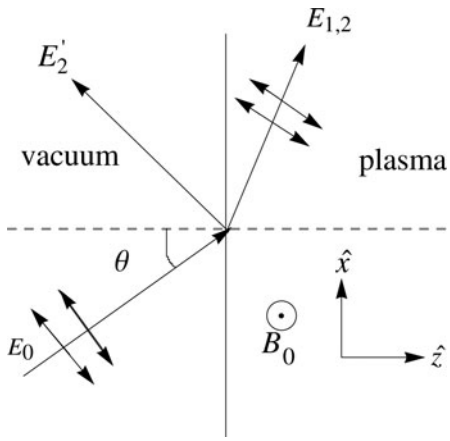

Fig. 1. Schematic representation of second-harmonic generation process.

https://doi.org/10.1017/S0263034617000544 Published online by Cambridge University Press

where **J** is the plasma electron current density. The governed equations on electron motion are given by the set of relativistic cold electron fluid equation

$$\frac{d(\gamma \boldsymbol{v})}{dt} = -\frac{e\mathbf{E}}{m} - \frac{e}{mc}\boldsymbol{v} \times (\mathbf{B} + \mathbf{B_0}), \tag{6}$$

and the continuity equation

$$\frac{\partial n}{\partial t} + \nabla.(n\boldsymbol{v}) = 0, \tag{7}$$

where γ is the relativistic factor, v and n are the velocity and density of plasma electrons, **B** and $\mathbf{B_0}$ are the magnetic fields corresponding to the radiation laser pulse and a self-generated magnetic field. We would like to start with perturbative theory and expand all quantities in orders of the radiation field amplitude. By making use of Eq. (6), the velocity components in the x and z directions are, respectively, given by

$$\frac{\partial v_{1x}}{\partial t} = -\frac{eE_x}{m} + \omega_c v_{1z}, \tag{8}$$

and

$$\frac{\partial v_{1z}}{\partial t} = \frac{eE_z}{m} - \omega_c v_{1x}, \tag{9}$$

where $\omega_c (= eB_0/mc)$ represents the cyclotron frequency and $E_{x,z} = E_{1(x,z)} + E_{2(x,z)}$ in which $E_{1(x,z)}$ and $E_{2(x,z)}$ are the amplitudes of electric field in fundamental and SH. By making use of Eqs (2)–(4), we can solve Eqs (8) and (9) to derive the first order of velocity components as

$$\begin{aligned} v_{1x} = &\left(\frac{i\omega_0^2 a_{1x} c}{\omega_c^2 - \omega_0^2} + \frac{\omega_0 \omega_c a_{1z} c}{\omega_c^2 - \omega_0^2}\right) e^{i(k_{1x}x + k_{1z}z - \omega_0 t)} \\ &+ \left(\frac{2i\omega_0^2 a_{2x} c}{\omega_c^2 - 4\omega_0^2} + \frac{\omega_0 \omega_c a_{2z} c}{\omega_c^2 - 4\omega_0^2}\right) e^{i(k_{2x}x + k_{2z}z - 2\omega_0 t)} + \text{c.c.}, \end{aligned} \tag{10}$$

$$\begin{aligned} v_{1z} = &\left(\frac{\omega_0 \omega_c a_{1x} c}{\omega_c^2 - \omega_0^2} - \frac{i\omega_0^2 a_{1z} c}{\omega_c^2 - \omega_0^2}\right) e^{i(k_{1x}x + k_{1z}z - \omega_0 t)} \\ &+ \left(\frac{\omega_0 \omega_c a_{2x} c}{\omega_c^2 - 4\omega_0^2} - \frac{2i\omega_0^2 a_{2z} c}{\omega_c^2 - 4\omega_0^2}\right) e^{i(k_{2x}x + k_{2z}z - 2\omega_0 t)} + \text{c.c.} \end{aligned} \tag{11}$$

Where $a_{j(x,z)} = eE_{j(x,z)}/m\omega_0 c$ ($j = 1,2$) are the components of normalized amplitude of the transmitted fundamental and SH electric field.

By following the same steps, the expression for velocity components in second order is given by

$$\frac{\partial v_{2x}}{\partial t} = \frac{e}{mc} v_{1z} B_{1y} - v_{1x}\frac{\partial v_{1x}}{\partial x} - v_{1z}\frac{\partial v_{1x}}{\partial z} + \omega_c v_{2z}, \tag{12}$$

and

$$\frac{\partial v_{2z}}{\partial t} = -\frac{e}{mc} v_{1x} B_{1y} - v_{1z}\frac{\partial v_{1z}}{\partial z} - v_{1x}\frac{\partial v_{1z}}{\partial x} - \omega_c v_{2x}. \tag{13}$$

The second-order velocity components are obtained by using of Eqs (10) and (11) and simultaneous solutions of Eqs (12) and (13) as bellow

$$\begin{aligned} v_{2x} = &\frac{\epsilon_1 a_1^2 \omega_0^2 c^2}{(\omega_c^2 - \omega_0^2)^2(\omega_c^2 - 4\omega_0^2)}\left[\frac{1}{\omega_0}(2\omega_0^4 - \omega_c^4 - 4\omega_0^2\omega_c^2)k_{1x}\right. \\ &\left. - i\omega_c(4\omega_c^2 - \omega_0^2)k_{1z}\right] e^{2i(k_{1x}x + k_{1z}z - \omega_0 t)} + \text{c.c.}, \end{aligned} \tag{14}$$

$$\begin{aligned} v_{2z} = &\frac{\epsilon_1 a_1^2 \omega_0^2 c^2}{(\omega_c^2 - \omega_0^2)^2(\omega_c^2 - 4\omega_0^2)}\left[i\omega_c(4\omega_c^2 - \omega_0^2)k_{1x}.\right. \\ &\left. + \frac{1}{\omega_0}(2\omega_0^4 - \omega_c^4 - 4\omega_0^2\omega_c^2)k_{1z}\right] e^{2i(k_{1x}x + k_{1z}z - \omega_0 t)} + \text{c.c.} \end{aligned} \tag{15}$$

Using Eq. (7), the first-order density perturbation is given as follows

$$\begin{aligned} n_1 = &\frac{n_0 a_1 \omega_c k_1^2 c^2}{\omega_0(\omega_c^2 - \omega_0^2)} e^{i(k_{1x}x + k_{1z}z - \omega_0 t)} \\ &+ \frac{n_0 a_2 \omega_c k_2^2 c^2}{4\omega_0(\omega_c^2 - 4\omega_0^2)} e^{i(k_{2x}x + k_{2z}z - 2\omega_0 t)} + \text{c.c.} \end{aligned} \tag{16}$$

We find from Eq. (16) that the density perturbation disappears in the absence of external magnetic field. The plasma current density $\mathbf{J} = -en\boldsymbol{v}$ components can be derived as

$$\begin{aligned} J_x = &-\frac{n_0 e\omega_0 c}{\omega_c^2 - \omega_0^2}(i\omega_0 a_{1x} + \omega_c a_{1z}) e^{i(k_{1x}x + k_{1z}z - \omega_0 t)} \\ &- \frac{n_0 e\omega_0 c}{\omega_c^2 - 4\omega_0^2}(2i\omega_0 a_{2x} + \omega_c a_{2z}) e^{i(k_{2x}x + k_{2z}z - 2\omega_0 t)} \\ &- \frac{n_0 ec\epsilon_1 a_1^2 \omega_0^2}{(\omega_c^2 - \omega_0^2)^2(\omega_c^2 - 4\omega_0^2)}\left[-3i\omega_c(\omega_0^2 + \omega_c^2)k_{1z}c\right. \\ &\left. + 2\omega_0(\omega_0^2 - 4\omega_c^2)k_{1x}c\right] e^{2i(k_{1x}x + k_{1z}z - \omega_0 t)} + \text{c.c.}, \end{aligned} \tag{17}$$

and

$$\begin{aligned} J_z = &-\frac{n_0 e\omega_0 c}{\omega_c^2 - \omega_0^2}(\omega_c a_{1x} - i\omega_0 a_{1z}) e^{i(k_{1x}x + k_{1z}z - \omega_0 t)} \\ &- \frac{n_0 e\omega_0 c}{\omega_c^2 - 4\omega_0^2}(\omega_c a_{2x} - 2i\omega_0 a_{2z}) e^{i(k_{2x}x + k_{2z}z - 2\omega_0 t)} \\ &- \frac{n_0 ec\epsilon_1 a_1^2 \omega_0^2}{(\omega_c^2 - \omega_0^2)^2(\omega_c^2 - 4\omega_0^2)}\left[2\omega_0(\omega_0^2 - 4\omega_c^2)k_{1z}c\right. \\ &\left. + 3i\omega_c(\omega_0^2 + \omega_c^2)k_{1x}c\right] e^{2i(k_{1x}x + k_{1z}z - \omega_0 t)} + \text{c.c.} \end{aligned} \tag{18}$$

Substituting the linear parts of current density into the wave equation, we get to the linear dispersion relations for fundamental and SH.

$$k_1^2 c^2 = \omega_0^2 - \frac{\omega_p^2(\omega_0^2 - \omega_p^2)}{\omega_0^2 - \omega_p^2 - \omega_c^2}, \tag{19}$$

https://doi.org/10.1017/S0263034617000544 Published online by Cambridge University Press

and

$$k_2^2c^2 = 4\omega_0^2 - \frac{\omega_p^2(4\omega_0^2 - \omega_p^2)}{4\omega_0^2 - \omega_p^2 - \omega_c^2}. \quad (20)$$

Equations (19) and (20) introduce the dispersion relation for extraordinary waves in fundamental and SH propagating perpendicular to the magnetic field.

3. SH GENERATION

In order to evaluate the amplitude of the SH field, the source currents, Eqs (17) and (18), can be used in the wave Eq. (5) and equate the SH terms on both sides,

$$\frac{\partial^2 a_{2x}(z)}{\partial z^2} + \chi_1 \frac{\partial a_{2x}(z)}{\partial z} + \chi_2 a_{2x}(z) + \chi_3 a_{2z}(z) = \chi_4 e^{i\Delta k.z}, \quad (21)$$

and

$$\frac{\partial^2 a_{2z}(z)}{\partial z^2} + \chi_1 \frac{\partial a_{2z}(z)}{\partial z} + \chi_2 a_{2z}(z) - \chi_3 a_{2x}(z) = \chi_5 e^{i\Delta k.z}, \quad (22)$$

where

$$\chi_1 = 2ik_{2z},$$
$$\chi_2 = \frac{\omega_c^2\omega_p^4}{c^2(4\omega_0^2 - \omega_c^2)(4\omega_0^2 - \omega_p^2 - \omega_c^2)},$$
$$\chi_3 = \frac{i\omega_c\omega_p^4(4\omega_0^2 - \omega_p^2)}{2\omega_0 c^2(4\omega_0^2 - \omega_c^2)(4\omega_0^2 - \omega_p^2 - \omega_c^2)},$$
$$\chi_4 = \frac{2\varepsilon_1 a_1^2\omega_0^2\omega_p^2}{c^2(\omega_c^2 - \omega_0^2)^2(\omega_c^2 - 4\omega_0^2)} \times \left[2i\omega_0(\omega_0^2 - 4\omega_c^2)k_{1x}c + 3\omega_c(\omega_0^2 + \omega_c^2)k_{1z}c\right],$$
$$\chi_5 = \frac{2\varepsilon_1 a_1^2\omega_0^2\omega_p^2}{c^2(\omega_c^2 - \omega_0^2)^2(\omega_c^2 - 4\omega_0^2)} \times \left[3\omega_c(\omega_0^2 + \omega_c^2)k_{1x}c - 2i\omega_0(\omega_0^2 - 4\omega_c^2)k_{1z}c\right].$$

In this case, the wavenumber of the SH is more than twice as large as that for the fundamental wave at which $\Delta k = 2k_{1z} - k_{2z}$ is called the wavevector mismatch for SH radiation. We assume that $\partial a_{2(x,z)}(z)/\partial z$ considerably changes larger than the laser wavelength, means that $\partial^2 a_{2(x,z)}(z)/\partial z^2 \ll k_{2z}\partial a_{2(x,z)}(z)/\partial z$, which is known as the slowly varying envelope approximation (SVEA) and is almost valid in non-linear processes. Furthermore, assuming $a_{1(x,z)}$ depletes very slightly with z so that the quantity $a_{1(x,z)}^2$ can be considered to be independent of z. Therefore, solution or Eqs (21) and (22) lead us to the normalized amplitudes for the phase-mismatch SH inside the plasma and vacuum as

$$a_{2x}(z) = \begin{cases} \left[a_{2x}(0)\cos\left(\frac{\chi_3}{\chi_1}z\right) - a_{2z}(0)\sin\left(\frac{\chi_3}{\chi_1}z\right) + \alpha\left(q_1\cos\left(\frac{\chi_3}{\chi_1}z\right)\right.\right. \\ \left.\left. + q_2\sin\left(\frac{\chi_3}{\chi_1}z\right) - q_1 e^{(\chi_2 + i\chi_1\Delta k/(\chi_1)z)}\right)\right] e^{(-(\chi_2/\chi_1)z)}, & z > 0, \\ A_{2r}, & z < 0, \end{cases} \quad (23)$$

and

$$a_{2z}(z) = \begin{cases} \left[a_{2z}(0)\cos\left(\frac{\chi_3}{\chi_1}z\right) + a_{2x}(0)\sin\left(\frac{\chi_3}{\chi_1}z\right) + \alpha\left(q_1\sin\left(\frac{\chi_3}{\chi_1}z\right)\right.\right. \\ \left.\left. - q_2\cos\left(\frac{\chi_3}{\chi_1}z\right) + q_2 e^{(\chi_2 + i\chi_1\Delta k/(\chi_1)z)}\right)\right] e^{(-(\chi_2/\chi_1)z)}, & z > 0, \\ A'_{2r}, & z < 0, \end{cases} \quad (24)$$

where

$$q_1 = \chi_3\chi_5 - \chi_2\chi_4 - i\chi_1\chi_4\Delta k,$$
$$q_2 = \chi_3\chi_4 + \chi_2\chi_5 + i\chi_1\chi_5\Delta k,$$
$$\alpha = \frac{1}{\chi_1\Delta k(2i\chi_2 - \chi_1\Delta k)},$$

Here A_{2r} and A'_{2r} are reflected SH amplitudes in x and z directions and $a_{2x}(0)$ and $a_{2z}(0)$ refer to the amplitudes of SH wave components at $z = 0$. Using $\nabla.a_2 = 0$ in the vacuum, we find $A'_{2r} = (k_{0x}/k_{0z})A_{2r}$. The magnetic field amplitude of the SH radiation derived as

$$B_{2y}(z) = \begin{cases} \frac{mc^2}{2ie}\left[ik_{2z}a_{2x}(z) + 2ik_{1x}a_{2z}(z) + e^{-(\chi_2/\chi_1)z}(-\varphi(z)a_{2x}(0)\right. \\ +\phi(z)a_{2z}(0) - \alpha[q_1(\varphi(z) + i\Delta k e^{(\chi_2 + i\chi_1\Delta k/(\chi_1)z)}) \\ \left.+q_2\phi(z)])\right], & z > 0, \\ -\frac{mc\omega_0}{e\cos\theta}A_{2r}, & z < 0, \end{cases} \quad (25)$$

where

$$\varphi(z) = \frac{\chi_2}{\chi_1}\cos\left(\frac{\chi_3}{\chi_1}z\right) + \frac{\chi_3}{\chi_1}\sin\left(\frac{\chi_3}{\chi_1}z\right),$$
$$\phi(z) = \frac{\chi_2}{\chi_1}\sin\left(\frac{\chi_3}{\chi_1}z\right) - \frac{\chi_3}{\chi_1}\cos\left(\frac{\chi_3}{\chi_1}z\right).$$

In order to obtain the amplitudes $a_{2x}(0)$, $a_{2z}(0)$, and A_{2r}, we apply the proper boundary conditions for electric and magnetic fields E_{2x} and B_{2y} and displacement vector εE_{2z} at $z = 0$. We get

$$A_{2r} = -a_{2x}(0), \quad (26)$$

https://doi.org/10.1017/S0263034617000544 Published online by Cambridge University Press

$$\frac{2i\omega_0}{c\cos(\theta)}A_{2r}+\left[\frac{\chi_2}{\chi_1}-ik_{2z}\right]a_{2x}(0)+\left[\frac{\chi_3}{\chi_1}-2ik_{1x}\right]a_{2z}(0)=\alpha\left[q_2\frac{\chi_3}{\chi_1}-q_1\left(\frac{\chi_2+i\chi_1\Delta k}{\chi_1}\right)\right]. \tag{27}$$

Integrating the Poisson equation $\nabla.\epsilon\mathbf{E}=-en_1$, we will get the following relation

$$\frac{k_{0x}}{k_{0z}}A_{2r}-\epsilon_2 a_{2z}(0)=-\frac{i\omega_c\omega_p^2k_2^2c}{32\pi k_{1x}\omega_0^2(4\omega_0^2-\omega_c^2)}a_2(0). \tag{28}$$

The right-hand side of Eq. (28) is very small for underdense plasma ($\omega_p^2/\omega_0^2\ll1$), and we can neglect from this term. Therefore, we obtain from the set of Eqs (26–28) the SH waves amplitudes at plasma surface as

$$a_{2x}(0)=-A_{2r}=\frac{\alpha[q_2(\chi_3/\chi_1)-q_1(\chi_2+i\chi_1\Delta k/\chi_1)]}{\chi_2/\chi_1-ik_{2z}-2i\omega_0/c\cos(\theta)-\tan(\theta)/\varepsilon_2(\chi_3/\chi_1-2ik_{1x})}, \tag{29}$$

and

$$a_{2z}(0)=\frac{\alpha\tan(\theta)/\epsilon_2[q_1(\chi_2+i\chi_1\Delta k/\chi_1)-q_2(\chi_3/\chi_1)]}{\chi_2/\chi_1-ik_{2z}-2i\omega_0/c\cos(\theta)-\tan(\theta)/\epsilon_2(\chi_3/\chi_1-2ik_{1x})}. \tag{30}$$

The well-known SH conversion efficiency (η) is given by

$$\eta=\frac{\mu_2}{\mu_1}\frac{|a_2|^2}{|a_1|^2}, \tag{31}$$

where $\mu_1=\sqrt{\epsilon_1}$ and $\mu_2=\sqrt{\epsilon_2}$ are the refractive indexes corresponding to the fundamental and SH radiations, respectively.

3.1 Normal incidence

It is straightforward to show that for normal incidence of laser pulse, the coefficients χ_2, χ_3, and χ_5 do not appear in differential Eqs (21) and (22). Furthermore, just the x component of SH wave and y component of wavevector exist. Therefore, coupled Eqs (21) and (22) reduce to an differential equation for laser field amplitude in x direction as bellow

$$\chi_1\frac{\partial a_2(z)}{\partial z}=\chi_4'e^{i\Delta k.z}, \tag{32}$$

where the coefficient χ_4 is changed to

$$\chi_4'=\frac{6k_1\omega_c\omega_0^2\omega_p^2a_1^2(\omega_0^2+\omega_c^2)}{c(\omega_c^2-\omega_0^2)^2(\omega_c^2-4\omega_0^2)}.$$

The detailed derivation of Eq. (32) is shown in Appendix. We obtain the transmitted SH radiation amplitude by solution of Eq. (32) at normal incidence as bellow

$$a_2(z)=a_2(0)-\frac{i\chi_4'}{k_2\Delta k}e^{i\Delta kz/2}\sin\left(\frac{\Delta k.z}{2}\right). \tag{33}$$

Following Eqs (23), (25)–(27), for normal incidence, $a_2(0)$ can be derived as bellow

$$a_2(0)=\frac{c\chi_4'}{2k_2(2\omega_0+k_2c)}. \tag{34}$$

Above equations show that the amplitude of SH radiation is different from previous report by Jha *et al*. (2007). This difference is due to the reflection of SH radiation from vacuum–plasma interface, and changes by plasma density, strength of magnetic field, and laser intensity. Furthermore, the reflected SH radiation amplitude at normal incidence is given by

$$a_2'=-\frac{c\chi_4'}{2k_2(2\omega_0+k_2c)}. \tag{35}$$

Therefore, we obtain conversion efficiencies of the SH in both sides of plasma boundary as

$$\eta(z>0)=\frac{c\chi_4'^2}{2\omega k_2a_0^2}\frac{\sin^2(\Delta k.z/2)}{\Delta k^2}+\frac{c\chi_4'a_2(0)}{\omega\Delta ka_0^2}\sin^2\left(\frac{\Delta k.z}{2}\right)+\frac{\sqrt{\epsilon_2}a_2^2(0)}{a_0^2}, \tag{36}$$

$$\eta(z<0)=\frac{9k_1^2\omega_c^2\omega_0^4\omega_p^4a_1^4(\omega_0^2+\omega_c^2)^2}{k_2^2a_0^2(\omega_c^2-4\omega_0^2)^2(2\omega_0+k_2c)^2(\omega_c^2-\omega_0^2)^4}. \tag{37}$$

It is obvious from Eq. (36), the first term is in complete agreement with Jha *et al*. (2007), and the second and third terms are obtained by taking into account the reflected SH components contribution.

3.2 Non-magnetized plasma

It is clear that in the absence of the magnetic field the coefficients of χ_2 and χ_3 are zero and the other coefficients change to

$$\chi_1=2ik_{2z},\quad \chi_4''=-\frac{i\epsilon_1k_{1x}a_1^2\omega_p^2}{\omega_0c},\quad \chi_5''=\frac{i\epsilon_1k_{1z}a_1^2\omega_p^2}{\omega_0c}.$$

In this case, the dispersion relations of fundamental and SH waves are expressed by Eqs (19) and (20) with $\omega_c=0$. After applying these changes in Eqs (23–30), the transmitted and reflected SH radiation amplitude are written as

https://doi.org/10.1017/S0263034617000544 Published online by Cambridge University Press

$$a_2(z) = \left[Ae^{i(\Delta k.z)} \sin^2\left(\frac{\Delta k.z}{2}\right) + iBe^{i\Delta k.z/2} \sin\left(\frac{\Delta k.z}{2}\right) - C \right]^{1/2}, \tag{38}$$

and

$$a_2' = \frac{i\omega_p^2 a_1^2 \epsilon_1 \epsilon_2 k_{1x}}{4\omega_0^2 k_{2z} D}, \tag{39}$$

where

$$A = \frac{\omega_p^4 a_1^4 \epsilon_1^3}{k_{2z}^2 \Delta k^2 c^4},$$

$$B = -\frac{\omega_p^4 a_1^4 \epsilon_1^2 k_{1x}^2 (\epsilon_2 k_{0z} + k_{1z})}{2\omega_0^4 k_{2z}^2 \Delta k D},$$

$$C = \frac{\omega_p^4 a_1^4 \epsilon_1^2 k_{1x}^2 c^2 (\epsilon_2^2 k_{0z}^2 + k_{1x}^2)}{16\omega_0^6 k_{2z}^2 D^2},$$

$$D = \frac{k_{1x}^2 c^2}{\omega_0^2} - \epsilon_2 \left(1 + \frac{k_{0z} k_{2z} c^2}{2\omega_0^2}\right).$$

We get the conversion efficiencies of the SH inside the plasma as well as vacuum as bellow:

$$\eta(z>0) = \left[\frac{\epsilon_2}{a_0^4} (A(A+2B)\sin^4\left(\frac{\Delta k.z}{2}\right) + (B(B+2C) - 2AC\cos(\Delta k.z))\sin^2\left(\frac{\Delta k.z}{2}\right) + C^2) \right]^{1/2}, \tag{40}$$

$$\eta(z<0) = \frac{\omega_p^4 a_0^2 \epsilon_1^4 \epsilon_2^2 \cos^4\theta \sin^2\theta (\sin^2\theta - \epsilon_2(1 + \cos\theta\sqrt{\epsilon_2 - \sin^2\theta}))^{-2}}{4\omega^4(\epsilon_2 - \sin^2\theta)(\epsilon_1\cos\theta + \sqrt{\epsilon_1 - \sin^2\theta})^4}. \tag{41}$$

It is obvious from Eq. (38), for $B = C = 0$, the SH efficiency is in complete agreement with Jha and Agrawal (2014).

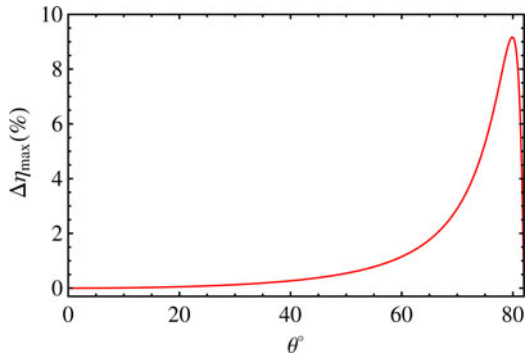

Fig. 3. Variation of $\Delta\eta_{max}$ as a function of incident angle θ. The parameters are chosen as $a_0 = 0.1$, $\omega_p/\omega_0 = 0.1$, and $\omega_c/\omega_0 = 0$.

It should be noted that, Eq. (40) is obtained by taking into account the reflected SH components contribution. Consequently, the introduced SH conversion efficiency by Eq. (40) is different with previous report in which the reflected SH contribution was missed (Jha & Agrawal, 2014). The order of deviation will be discussed in the next section.

4. NUMERICAL RESULTS

In this section, we would like to determine the conversion of a fraction of a laser beam to its phase-mismatch SH. To do this, we consider the pump laser a Nd:Yag with intensity $I_0 \leq 10^{17}\,\mathrm{W/cm^2}$ $(a_0 \leq 0.3)$ and frequency $\omega_0 = 1.88 \times 10^{15}\,\mathrm{rad/s}$ and or wavelength $\lambda = 1\,\mu\mathrm{m}$.

Figure 2 depicted variation of conversion efficiency (η%) with respect to the normalized propagation distance z/λ. Figure 2 shows that the conversion efficiency is periodic in z for a given value of Δk, so we have the points with maximum and minimum electric field amplitudes for the SH radiation. The maximum power efficiency (η_{max}) takes place in the coherence length $z_c = \pi/\Delta k$. In Figure 2a, 2b, the red dashed and black dotted lines are plotted based on the previous report (Jha & Agrawal, 2014) and Eq. (40), in the absence of magnetic field, respectively. It seems from the figure that for incidence angle near the critical, the deviation

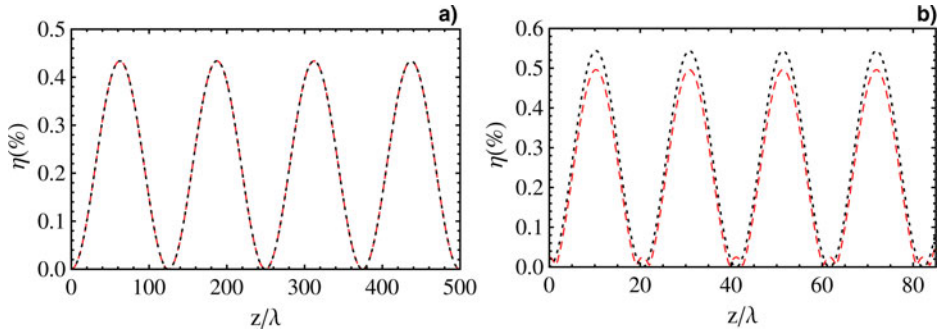

Fig. 2. Variation of transmitted second-harmonic conversion efficiency (η%) as a function of normalized propagation distance z/λ for different values of incidence angle (a) $\theta = 20$ and (b) $\theta = 80$ ($\theta \approx \theta_c$). The previous report (Jha & Agrawal, 2014) (dotted line) is compared with our result in the absence of the magnetic field (dashed line), respectively. The other parameters are $a_0 = 0.1$, $\omega_p/\omega_0 = 0.1$.

https://doi.org/10.1017/S0263034617000544 Published online by Cambridge University Press

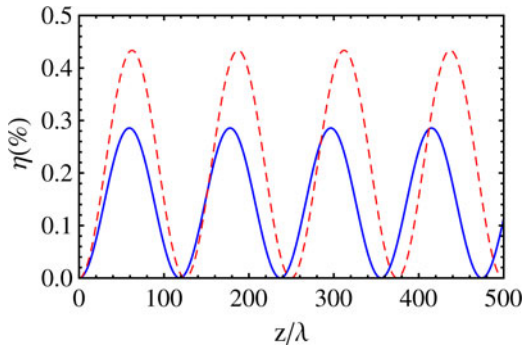

Fig. 4. Variation of transmitted second-harmonic conversion efficiency (η%) as a function of normalized propagation distance z/λ. The dashed and solid lines are plotted for non-magnetized and magnetized $\omega_c/\omega_0 = 0.2$ ($B_0 = 22MG$) plasmas, respectively. The other parameters are $\omega_p/\omega_0 = 0.1$ and $\theta = 20$.

increases; however, for angle far from the critical (Fig. 2a), our result is in complete agreement with previous report.

In Figure 3, we plotted the relative difference of the maximum efficiency ($\Delta\eta_{max} = |\eta'_{max} - \eta_{max}|/\bar{\eta}_{max}$), where η'_{max} and η_{max} refer to the maximum efficiencies reported based on Jha and Agrawal (2014) and Eq. (40) also $\bar{\eta}_{max} = (\eta'_{max} + \eta_{max})/2$, as a function of incidence angle. We found from the figure that the deviation reaches to the maximum around 10%, near to the critical angle. The results show that deviation depends strongly to the laser field intensity and plasma density, too. For example, for $a_0 = 0.3$ and plasma density near $\omega_p/\omega_0 = 0.5$, deviation can be increased up to the 36%, which is considerably large.

Figure 4 reveals the influence of self-generated transverse magnetic field on the SH power. The figure indicates SH variation in terms of the normalized propagation distance z/λ. The dashed and solid lines are plotted for a non-magnetized and a magnetized plasma, respectively. It is understood that the maximum conversion efficiency is decreased by magnetic field. Taking into account this fact that such strong magnetic fields can be generated in laser plasma interaction, therefore, we expect that in a real physical system, the SH power becomes less than the power reported for a non-magnetized plasma (Jha & Agrawal, 2014).

We compare SH conversion efficiency for normally and obliquely incident of a laser pulse on vacuum–plasma interface in Figure 5, in terms of the self-generated magnetic field strength ω_c/ω_0. Figure 5a is in complete agreement with previous report (Jha *et al.*, 2007). It seems that the magnetic field intensifies the SH power for normal incidence of a laser pulse, while SH power is weakened by magnetic field for obliquely incident. Moreover, Figure 5 clearly shows that the order of SH power is ten times greater for obliquely

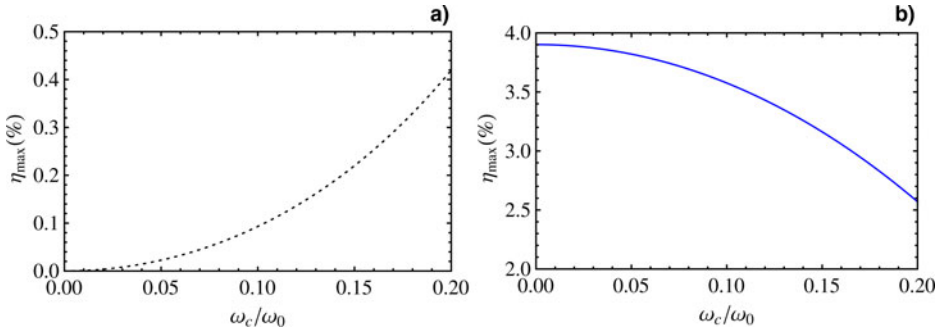

Fig. 5. Variation of maximum conversion efficiency (η_{max}%) as a function of magnetic field strength ω_c/ω_0 for $a_0 = 0.3$, $\omega_p/\omega_0 = 0.1$, (a) for normal incidence, and (b) for oblique incidence $\theta = 20$.

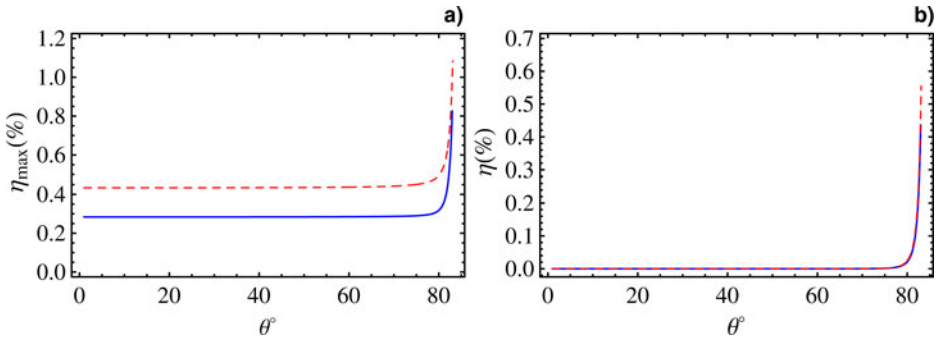

Fig. 6. Variations of (a) transmitted maximum conversion efficiency (η_{max}%) and (b) reflected conversion efficiency (η%), as a function of incidence angle for $a_0 = 0.1$, $\omega_p/\omega_0 = 0.1$ and different values of magnetic field strength. The dashed and solid lines are plotted for $B_0 = 0$ and 22 MG, respectively.

https://doi.org/10.1017/S0263034617000544 Published online by Cambridge University Press

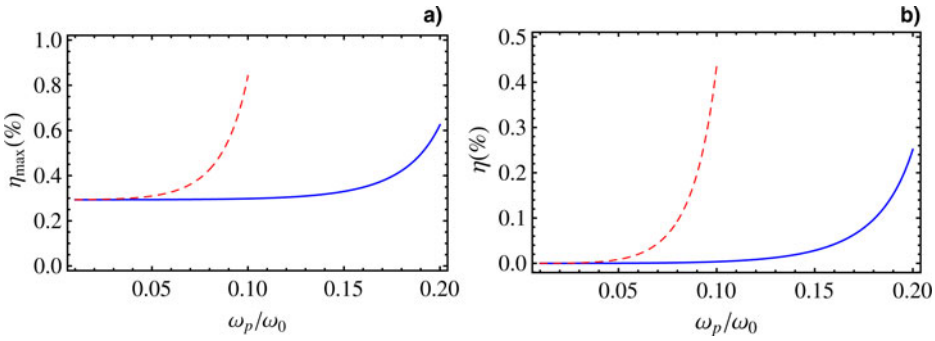

Fig. 7. Variations of (a) transmitted maximum conversion efficiency ($\eta_{max}\%$) and (b) reflected conversion efficiency ($\eta\%$), as a function of ω_p/ω_0 for $a_0 = 0.1$ and $B_0 = 22$ MG for different values of incident angle. The dashed and solid lines are plotted for $\theta = 83$ and 77, respectively.

incident. Figure 5a demonstrates that the magnetic field is essentially required for SH generation in normal incidence of a laser pulse on plasma surface (Jha *et al.*, 2007).

Figure 6 shows variations of transmitted maximum conversion efficiency ($\eta_{max}\%$) and reflected conversion efficiency ($\eta\%$) in terms of incident angle varying from $\theta \approx 0^{\circ}$ up to critical angle for different values of ω_c/ω_0. The solid and dashed lines are plotted for a magnetized and non-magnetized plasmas. Figure 6a shows that the SH power is smaller in a magnetized plasma. As the figures show that the efficiency of SH radiation increases very smoothly with incidence angle, however, it drastically increases near the critical angle. Figure 6b indicates that the influence of magnetic field, on the reflected SH power, is very poor and just near the critical angle a minor decrement (≈1%) is observable.

In Figure 7, we plotted variations of transmitted maximum conversion efficiency ($\eta_{max}\%$) and reflected conversion efficiency ($\eta\%$) as a function of plasma density ω_p/ω_0 for different values of incident angle. This figure predicts that for a given angle of incidence θ and magnetic field strength, the SH power sharply increases for both transmitted and reflected components when the plasma density satisfies the required condition $\theta \approx \theta_c$. For example, for given parameters in Figure 7, the condition $\theta \approx \theta_c$ is satisfied for angles $\theta = 83^{\circ}$ and $\theta = 77^{\circ}$ in plasma densities $\omega_p/\omega_0 \approx 0.1$ and $\omega_p/\omega_0 \approx 0.2$, respectively. We find from the Figures 6 and 7, the transmitted SH power is more than twice with respect to the reflected component; however, reflected component is more appropriate for technical and experimental applications.

5. SUMMERY AND CONCLUSION

In conclusion, we investigated the possibility of SH generation in the interaction of an obliquely *p*-polarized laser pulse on a vacuum-magnetized plasma interface. In view of this fact that strong megagauss magnetic fields can be generated in a laser plasma interaction, we modeled the self-generated magnetic field as a transverse magnetic field. We focused our attention to transmitted as well as reflected SH components. We shown that if the transmitted and reflected SH are considered as a simultaneous process, the results deviated from previous reports, especially near the critical angle (Jha *et al.*, 2007; Jha & Agrawal, 2014). The deviation can be increased by laser intensity and plasma density. Our analysis revealed a sharp increase for both transmitted and reflected SH components near the critical angle. We have demonstrated that transverse magnetic field had destructive role and the SH power decreased slightly with magnetic field strength enhancement. The analytical investigations show that the transmitted and reflected SH amplitudes are proportional to laser intensity ($I \propto a_1^2$), which as expected. If we kept the angel of incident and magnetic field strength constant and changed the plasma density, we found that the SH power for both transmitted and reflected components sharply intensified when the angle of incidence satisfied the required condition $\theta \approx \theta_c$. In view of this fact that the critical angle reduced by increasing plasma density, for a large incident angle the maximum power is generated at smaller plasma density. A comparison between transmitted and reflected SH revealed that the conversion efficiency is more than twice for transmitted component; however, the reflected component is more proper for technical and experimental applications.

REFERENCES

Askari, H.R. & Azish, Z. (2011). Effect of a periodic magnetic field on phase matching condition in second harmonic generation at interactions of laser-plasma. *Optik* **122**, 1159–1163.

Askari, H.R. & Noroozi, M. (2009). Effect of a wiggler magnetic field and the ponderomotive force on the second harmonic generation in laser-plasma interactions. *Phys. Turk* **33**, 299.

Berezhiani, V.I., Mahajan, S.M. & Shatashvili, N.L. (1997). Theory of magnetic field generation by relativistically strong laser radiation. *Phys. Rev. E* **55**, 995.

Cairns, R.A. (2009). The spectrum of second harmonic emission from a laser-produced plasma. *Laser Part. Beams* **22**, 149.

Esarey, E., Ting, A., Sprangle, P., Umstadter, D. & Liu, X. (1993). Nonlinear analysis of relativistic harmonic generation by intense lasers in plasmas. *IEEE Trans. Plasma. Sci.* **21**, 95.

Földes, I.B., Kocsis, G., Rácz, E., Szatmári, S. & Veres, G. (2003). Generation of high harmonics in laser plasmas. *Laser Part. Beams* **21**, 517.

https://doi.org/10.1017/S0263034617000544 Published online by Cambridge University Press

Franken, P.A., Hill, A.E., Peters, C.W. & Weinreich, G. (1961). Generation of optical harmonics. *Phys. Rev. Lett.* **7**, 118.

Ghorbanalilu, M. (2012). Second and third harmonics generation in the interaction of strongly magnetized dense plasma with an intense laser beam. *Laser Part. Beams* **30**, 291.

Giulietti, D., Banfi, G.P., Deha, I., Giulietti, A., Lucchesi, M., Nocera, L. & Zun, C.Z. (2009). Second harmonic generation in underdense plasma. *Laser Part. Beams* **6**, 141.

Gorbunov, L.M., Mora, P. & Antonsen, T.M. (1997). Quasistatic magnetic field generated by a short laser pulse in an underdense plasma. *Phys. Plasmas* **4**, 4358.

Grebogi, C., Tripathi, V.K. & Chen, H.H. (1983). Harmonic generation of radiation in a steep density profile. *Phys. Fluids* **26**, 1904.

Jha, P. & Agrawal, E. (2014). Second harmonic generation by propagation of a p-polarized obliquely incident laser beam in underdense plasma. *Phys. Plasmas* **21**, 053107.

Jha, P., Mishra, R.K., Raj, G. & Upadhyay, A.K. (2007). Second harmonic generation in laser magnetized-plasma interaction. *Phys. Plasmas* **14**, 053107.

Kant, N. & Sharma, A.K. (2004). Resonant second-harmonic generation of a short pulse laser in a plasma channel. *J. Phys. D: Appl. Phys.* **37**, 2395–2398.

Kant, N. & Thakur, V. (2016). Second harmonic generation by a chirped laser pulse in magnetized-plasma. *Optik* **127**, 4167–4172.

Kato, S., Nakamura, T., Mima, K., Sentoku, Y., Nagatomo, H. & Owadano, Y. (2004). Generation of quasistatic magnetic field in the relativistic laser-plasma interactions. *J. Plasmas Fusion Res. SERIES* **6**, 658–661.

Klein, M.W., Wegener, M., Feth, N. & Linden, S. (2007). Experiments on second- and third-harmonic generation from magnetic metamaterials. *Opt. Express* **15**, 5238–5247.

Kuri, D.K. & Das, N. (2016). Second-harmonic generation by an obliquely incident s-polarized laser from a magnetized plasma. *Laser Part. Beams* **34**, 276–283.

Lehner, T. (1994). Intense magnetic field generation by relativistic ponderomotive force in an underdense plasma. *Phys. Scr.* **49**, 704–711.

Li, G., Ni, J., Xie, H., Zeng, B., Yao, J., Chu, W., Zhang, H., Jing, C., He, F., Xu, H., Cheng, Y. & Xu, Z. (2014). Second harmonic generation in a centrosymmetric gas medium with spatiotemporally focused intense femtosecond laser pulses. *Opt. Lett.* **39**, 961–964.

Mori, M., Shiraishi, T., Abe, H., Taki, S., Kawada, Y. & Kondo, K. (2002). Image of second harmonic emission generated from ponderomotively excited plasma density gradient. *Phys. Plasmas* **9**, 2812.

Ondarza-Rovira, R. & Boyd, T.J.M. (2000). Plasma harmonic emission from laser interactions with dense plasma. *Phys. Plasmas* **7**, 1520.

Parashar, J. & Sharma, A.K. (1998). Second-harmonic generation by an obliquely incident laser on a vacuum-plasma interface. *Europhys. Lett.* **41**, 389–394.

Racz, E., Foldes, I.B., Kocsis, G., Veres, G., Eidmann, K. & Szatmri, S. (2006). On the effect of surface rippling on the generation of harmonics in laser plasmas. *Appl. Phys. B* **82**, 13–18.

Sharma, P. & Sharma, R.P. (2012). Study of second harmonic generation by high power laser beam in magneto plasma. *Phys. Plasmas* **19**, 122106.

Singh, K.P., Gupta, D.N., Yadav, S. & Tripathi, V.K. (2005). Relativistic second-harmonic generation of a laser from underdense plasma. *Phys. Plasmas* **12**, 013101.

Vaziri (Khamedi), M., Sohailya, S. & Bahrampour, A. (2015). Resonant second harmonic generation in plasma by self-focused twisted beam. *Opt. Commun.* **341**, 295–301.

Yeung, M., Rykovanov, S., Bierbach, J., Li, L., Eckner, E., Kuschel, S., Woldegeorgis, A., Rödel, C., Sävert, A., Paulus, G.G., Coughlan, M., Dromey, B. & Zepf, M. (2017). Experimental observation of attosecond control over relativistic electron bunches with two-colour fields. *Nat. Photonics* **11**, 32–35.

Zheng, C.Y., Zhu, S.P. & He, X.T. (2000). Quasistatic magnetic field generation by an intense ultrashort laser pulse in underdense plasma. *Chin. Phys. Lett.* **17**, 746.

APPENDIX A. DERIVATION OF SECOND HARMONIC RADIATION AMPLITUDE AT NORMAL INCIDENCE

A *p*-polarized laser beam incidents on the interface normally as follow

$$\mathbf{E}_0 = \hat{x}\frac{1}{2}E_0 \exp[i(k_0 z - \omega_0 t)] + \text{c.c.} \tag{A.1}$$

The electric and magnetic fields of the transmitted laser can be written as

$$\mathbf{E}_1 = \hat{x}\frac{1}{2}E_1 \exp[i(k_1 z - \omega_0 t)] + \text{c.c.}, \tag{A.2}$$

$$\mathbf{B}_1 = c\mathbf{k}_1 \times \mathbf{E}_1/\omega_0, \tag{A.3}$$

where $E_1 = 2E_0/1 + \sqrt{\epsilon_1}$ is the amplitude of the fundamental electric field transmitted into the plasma. The SH electric field can be written as

$$\mathbf{E}_2 = \hat{x}\frac{1}{2}E_2 \exp[i(k_2 z - 2\omega_0 t)] + \text{c.c.}, \tag{A.4}$$

Using Eq. (6), the first order of velocity components in the x and z directions are, respectively, given by

$$v_{1x} = \frac{i\omega_0^2 c}{\omega_c^2 - \omega_0^2} a_1 e^{i(k_1 z - \omega_0 t)} + \frac{2i\omega_0^2 c}{\omega_c^2 - 4\omega_0^2} a_2 e^{i(k_2 z - 2\omega_0 t)} + \text{c.c.}, \tag{A.5}$$

$$v_{1z} = \frac{\omega_0 \omega_c c}{\omega_c^2 - \omega_0^2} a_1 e^{i(k_1 z - \omega_0 t)} + \frac{\omega_0 \omega_c c}{\omega_c^2 - 4\omega_0^2} a_2 e^{i(k_2 z - 2\omega_0 t)} + \text{c.c.} \tag{A.6}$$

By following the same steps, the expression for the second-order transverse velocity are given by

$$v_{2x} = -\frac{i\omega_c k_1 a_1^2 \omega_0^2 c^2 (4\omega_c^2 - \omega_0^2)}{(\omega_c^2 - \omega_0^2)^2 (\omega_c^2 - 4\omega_0^2)} e^{2i(k_1 z - \omega_0 t)} + \text{c.c.} \tag{A.7}$$

By using Eq. (7), the first-order plasma electron density is

https://doi.org/10.1017/S0263034617000544 Published online by Cambridge University Press

given as follows

$$n_1 = \frac{n_0 a_1 \omega_c k_1 c}{(\omega_c^2 - \omega_0^2)} e^{i(k_1 z - \omega_0 t)} + \frac{n_0 a_2 \omega_c k_2 c}{2(\omega_c^2 - 4\omega_0^2)} e^{i(k_2 z - 2\omega_0 t)} + \text{c.c.} \quad \text{(A.8)}$$

The transverse current density can be derived by using electron density and velocity as follows

$$J_x = -\frac{in_0 e\omega_0^2 c}{\omega_c^2 - \omega_0^2} a_1 e^{i(k_1 z - \omega_0 t)} - \frac{2in_0 ec\omega_0^2}{\omega_c^2 - 4\omega_0^2} a_2 e^{i(k_2 z - 2\omega_0 t)} + \frac{3in_0 e\omega_c k_1 c^2 \omega_0^2 a_1^2 (\omega_0^2 + \omega_c^2)}{(\omega_c^2 - \omega_0^2)^2 (\omega_c^2 - 4\omega_0^2)} e^{2i(k_z z - \omega_0 t)} + \text{c.c.} \quad \text{(A.9)}$$

By substituting the current density into the wave Eq. (5), we obtain the following expressions

$$k_1^2 c^2 = \omega_0^2 - \frac{\omega_0^2 \omega_p^2}{\omega_0^2 - \omega_c^2}, \quad \text{(A.10)}$$

and

$$k_2^2 c^2 = 4\omega_0^2 - \frac{4\omega_0^2 \omega_p^2}{4\omega_0^2 - \omega_c^2}. \quad \text{(A.11)}$$

In order to determine the amplitude of SH field, Eq. (A.9) can be used in Eq. (5). We arrive

$$\frac{\partial^2 a_2(z)}{\partial z^2} + \chi_1 \frac{\partial a_2(z)}{\partial z} = \chi_4' e^{i\Delta k.z}, \quad \text{(A.12)}$$

where $\Delta k = 2k_1 - k_2$. Using SVEA approximation in above equation, we found

$$\chi_1 \frac{\partial a_2(z)}{\partial z} = \chi_4^{'} e^{i\Delta k.z}. \quad \text{(A.13)}$$

https://doi.org/10.1017/S0263034617000544 Published online by Cambridge University Press